Journal Name

ARTICLE TYPE

Cite this: DOI: 00.0000/xxxxxxxxxx

Supporting Information for: Stimuli-Responsive Polyelectrolyte Surfactant Complexes for the Reversible Control of Solution Viscosity

Giuseppe Rosario Del Sorbo,[a,b] Daniel Clemens,[c] Emanuel Schneck,*[d] and Ingo Hoffmann*[a,b]

Received Date
Accepted Date

DOI: 00.0000/xxxxxxxxxx

S I Materials

To understand how the monoanionic and dianonic species of SDP are distributed as a function of pH, the titration curve was determined, fig. S1. The curve shows two different regions: the first one in a pH range of 6-8 and a second in a range of 11-12. According with Nakayama *et al.* [1] at higher pH values the surfactant head groups are completely ionized (SDP^{2-}), while in solutions closed to neutrality mono charged species are present (SDP^{-}). The charge of the head gropup, which depends on the pH, dictates the aggregation behaviour of the pure surfactant solution. Large size aggregates are formed by protonated SDP molecules, while smaller size is constructed in alkaline solution due to the electrostatic head group repulsion which are bearing two negative charges [1,2].

To switch the pH back and forth for fig. 2, both NaOH (10 M solution) and HCl (1 M solution) were added from an Eppendorf pipette under vigorous stirring of the PESC solution. As the PESCs are shear thinning, the solution to which the NaOH is added is rather liquid so that mixing is not a problem even though the solution is quite viscous at rest. In the last step, the solution is diluted by about 10 % which ensures that the solution is still above the overlap concentration of JR 400 of about 0.8 wt% and it should also be noted that even at a PE concentration of 0.5 wt% a significant increase in viscosity could still be observed for JR 400 and sodium dodecylbenzenesulphonate [3]

S II Rheology

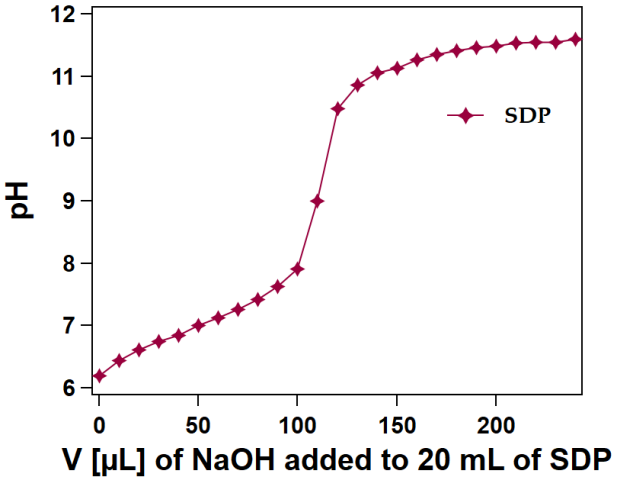

Fig. S1 Titration curve for SDP, 20 mM, at room temperature, in water as function of added volume of NaOH 0.1 M.

According to Green and Tobolsky [4,5], the plateau value of G', termed G_0, is related to the network junction density via:

$$G_0 = g\varepsilon k_B T \tag{S1}$$

with the network junction density ε, the absolute temperature T, Boltzmann's constant k_B and a factor g to account for the strength of the junctions in units of $k_B T$, which is initially set to 1 for the calculation of the values in table S I.

S III SANS

[a] *Max Planck Institute of Colloids and Interfaces, Am Mühlenberg 1, D-14476 Potsdam, Germany*
[b] *Institut Max von Laue-Paul Langevin (ILL), 71 avenue des Martyrs, CS 20156, F-38042 Grenoble Cedex 9, France; E-mail: hoffmann@ill.fr*
[c] *Helmholtz-Zentrum Berlin, Hahn-Meitner Platz 1, D-14109, Berlin, Germany*
[d] *Department of Physics, Technische Universität Darmstadt, Hochschulstraße 8, D-64289 Darmstadt, Germany; E-mail: emanuel.schneck@pkm.tu-darmstadt.de*

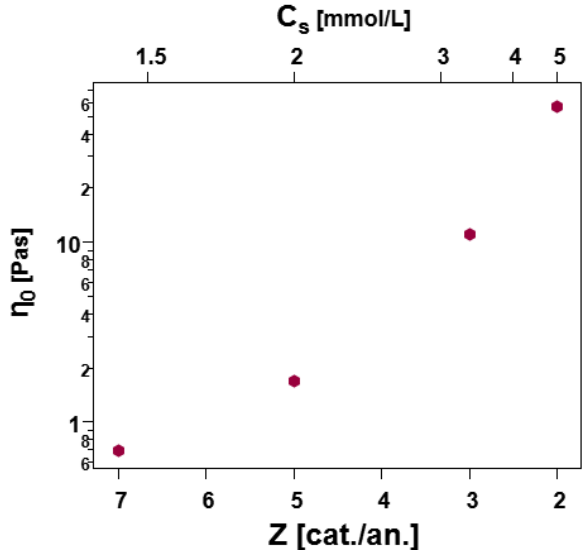

Fig. S2 Zero shear viscosity of JR 400/SDP^{-} mixtures as function of Z (bottom) and surfactant concentration (top).

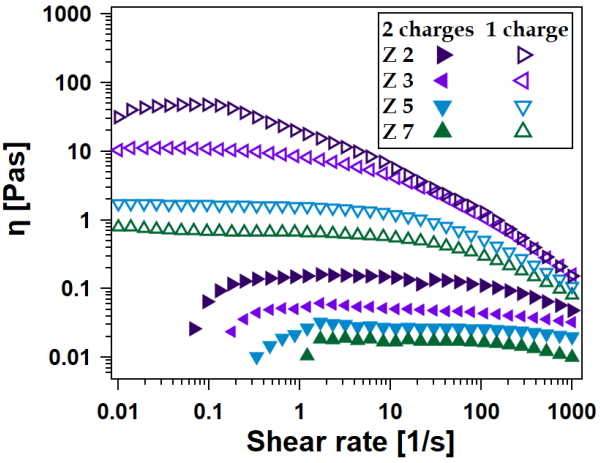

Fig. S3 Viscosity as a function of $\dot{\gamma}_{crit}$ of JR 400 with SDP^{2-} (closed symbols) and with SDP^{-} (open symbols) at different Z values

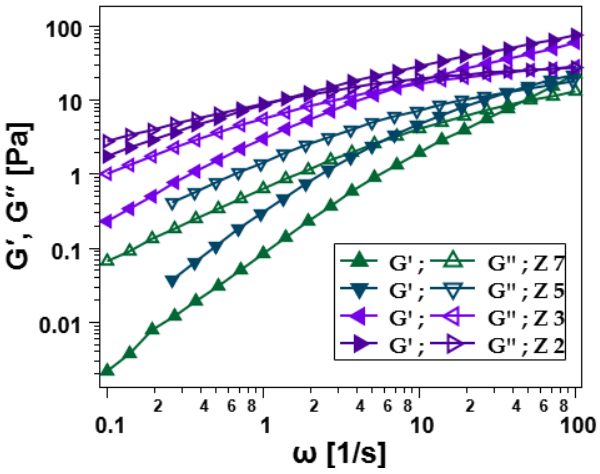

Fig. S4 Elastic modulus G' and viscous modulus G'' as a function of angular frequency for JR 400/SDP^{-} mixtures.

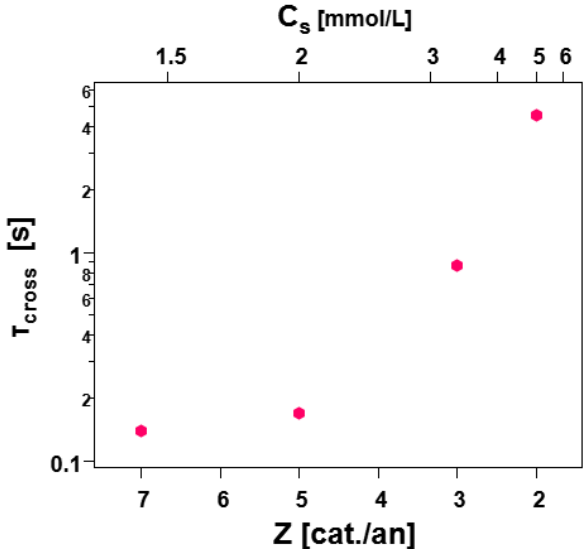

Fig. S5 Structural relaxation time τ_{cross} of JR 400/SDP^{-} as a function of Z (bottom) and surfactant concentration (top).

Table S I Parameters obtained from Oscillatory Shear Rheology of JR 400/SDP^{-} mixtures.

Z /	ω_{cross} [rad/s]	τ_{cross} [s]	G_0 [Pa]	ε [m^{-3}]	ξ [nm]
7	45	0.14	22	5.49 x 10^{21}	57
5	36	0.17	56	1.35 x 10^{22}	42
3	7.2	0.87	60	1.47 x 10^{22}	40
2	1.39	4.52	77	1.87 x 10^{22}	38

The SANS signal of an ensemble of monodisperse, non-interacting particles is generally given as:

$$I(Q) = {}^1N P(Q) + I_{\mathrm{bkg}} \tag{S2}$$

where ${}^1N$ is the particle number density, $P(Q)$ the particle form factor, and I_{bkg} the Q-independent, incoherent background which is subtracted in the curves shown in this manuscript. The form factor is defined such that $P(Q=0) = V_{\mathrm{p}}^2(\Delta\rho)^2$, where V_{p} is the volume of a particle and $\Delta\rho = \rho_{\mathrm{p}} - \rho_{\mathrm{m}}$ is the scattering length density difference between a particle and the surrounding medium. ${}^1N$ is coupled to the volume fraction ϕ and the particle volume V_{p} by ${}^1N = \phi/V_{\mathrm{p}}$.

The form factor of randomly oriented cylinders with radius R and length L is given by

$$P_{\mathrm{cyl}}(Q) = \int_0^1 F_{\mathrm{cyl}}(Q,x)^2 \mathrm{d}x, \tag{S3}$$

where the integral over x takes into account the orientational average and $F_{\mathrm{cyl}}(Q,x)$ is the scattering amplitude

$$F_{\mathrm{cyl}}(Q,x) = \pi R^2 L \Delta\rho \frac{4J_1(q,R\sqrt{1-x^2})\sin(qLx/2)}{q^2 R\sqrt{1-x^2}Lx} \tag{S4}$$

comprising the first order Bessel function J_1.

If the sample is polydisperse with regard to the radius, eq. (S2) takes the form

$$I(Q) = {}^1N \int_0^\infty f(R)P(Q,R)\mathrm{d}R + I_{\mathrm{bkg}} \tag{S5}$$

where $f(R)$ is the radius distribution and ${}^1N$ takes the form

$${}^1N = \frac{\phi}{\int_0^\infty f(R)V_{\mathrm{p}}(R)\mathrm{d}R}. \tag{S6}$$

Here, we used the normalised lognormal distribution function

$$f(R,R\mathrm{m},\sigma) = \frac{1}{\sqrt{2\pi}\sigma R}\exp\left(-\frac{\ln(R/R_{\mathrm{m}})^2}{2\sigma^2}\right) \tag{S7}$$

$$M = R_{\mathrm{m}}\exp\left(\frac{1}{2\sigma^2}\right) \tag{S8}$$

where M is the mean value of the distribution and the standard deviation is given by $\sqrt{\exp(\sigma^2)-1}R_{\mathrm{m}}\exp(1/2\sigma^2)$, fixed at 10%. The curve of pure PE can be described by the equation:

$$I_{\mathrm{PE}}(Q) = {}^1N_{\mathrm{PE}} \int f(R,R_{\mathrm{PE}})P_{\mathrm{cyl}}(Q,R,\Delta\rho_{\mathrm{PE}},L_{\mathrm{PE}})\mathrm{d}R, \tag{S9}$$

with the scattering length density difference $\Delta\rho_{\mathrm{PE}}$ between PE and D_2O and the particle number density of free PE segments

$${}^1N_{\mathrm{PE}} = \frac{\phi_{\mathrm{PE}}}{\int f(R,R_{\mathrm{PE}},\sigma)V(R,L)\mathrm{d}R}. \tag{S10}$$

The SANS curves of PE/SDP^{2-}, see fig. S7, can be described with the same model used for the pure PE, only adapting the volume fraction and the scattering length density, so that

$$\phi_{\mathrm{PE/SDP^{2-}}} = \phi_{\mathrm{PE}} + y_{\mathrm{SDP^{2-}}}\cdot\phi_{\mathrm{SDP^{2-}}} \tag{S11}$$

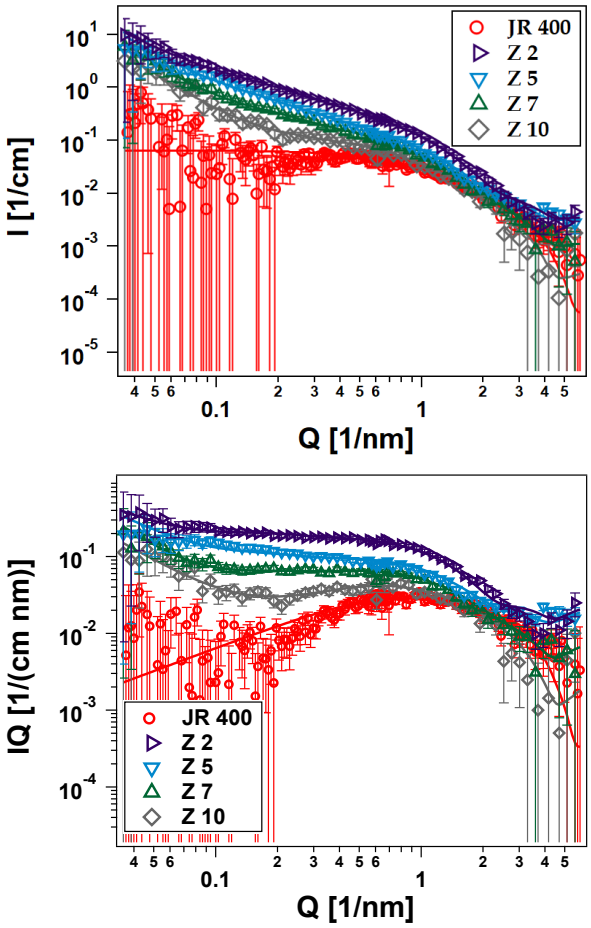

Fig. S6 Comparison of the SANS curves of 1 wt% JR 400 with SDP$^-$ at different Z values and pure JR 400. Raising the surfactant concentration (*i.e.*, reducing Z), an increase of the scattering intensity without a change of the shape of the curve is observed at high Q, because of the formation of mixed aggregates. Top: As Intensity vs Q plot; bottom: as Holtzer plot

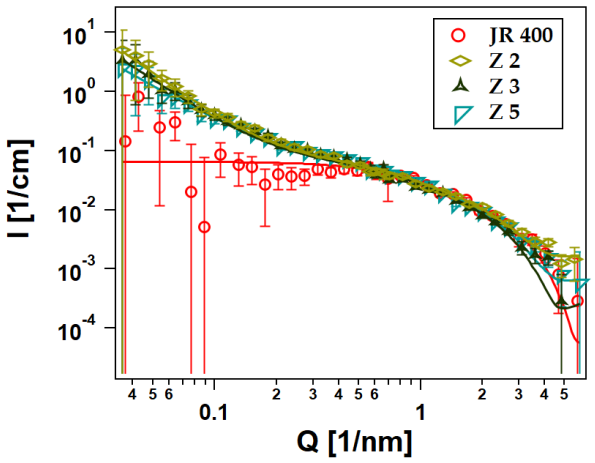

Fig. S7 SANS curves of JR 400/SDP^{2-} 1 wt % at different charge ratios.

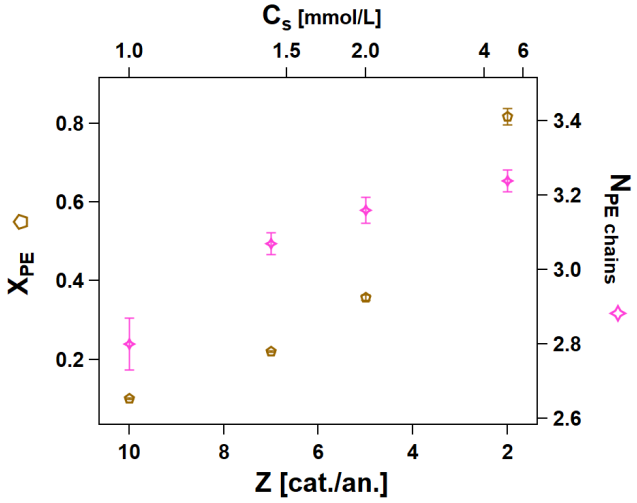

Fig. S8 Fraction of PE in the aggregates x_{PE}, left axis. Average number of PE chains per aggregate, right axis. Both as a function of charges ratio (bottom) and SDP^{2-} concentration (top).

and

$$\rho_{\mathrm{PE/SDP^{2-}}} = \frac{\phi_{\mathrm{PE}}}{\phi_{\mathrm{PE/SDP^{2-}}}}\rho_{\mathrm{PE}} + \frac{y_{\mathrm{SDP^{2-}}}\phi_{\mathrm{SDP^{2-}}}}{\phi_{\mathrm{PE/SDP^{2-}}}}\rho_{\mathrm{SDP^{2-}}} \tag{S12}$$

To describe the PE/SDP^{2-} mixed aggregates (see fig. 4), it has been used the fallow equation[6,7]:

$$\begin{aligned} I_{\mathrm{agg}}(Q) = {}^{1}N_{\mathrm{agg}} &\int f(R,R_{\mathrm{agg}},\sigma)P_{\mathrm{cyl}}(Q,R,\Delta\rho_{\mathrm{agg}},L_{\mathrm{agg}})\mathrm{d}R \\ &+ \mathrm{erf}\left(\left(QR_{\mathrm{agg}}/\sqrt{12}\right)^2\right)\frac{\phi_{\mathrm{PE}}x_{\mathrm{PE}}}{\int f(R,R_{\mathrm{PE}},\sigma)V_p(R,L_{\mathrm{PE}})\mathrm{d}R} \\ &\times \int f(R,R_{\mathrm{PE}},\sigma)P_{\mathrm{cyl}}(Q,R,\rho_{\mathrm{PE}}-\rho_{\mathrm{surf}},L_{\mathrm{PE}})\mathrm{d}R \end{aligned} \tag{S13}$$

with the scattering length density of the aggregates ρ_{agg} given by:

$$\rho_{\mathrm{agg}} = \frac{\phi_{\mathrm{surf}}}{\phi_{\mathrm{agg}}}\rho_{\mathrm{surf}} + \frac{\phi_{\mathrm{PE}}x_{\mathrm{PE}}}{\phi_{\mathrm{agg}}}\rho_{\mathrm{PE}}. \tag{S14}$$

Assuming the aggregates homogeneous along their length it is possible to calculate the number of PE chains per aggregate via:

$$N_{\mathrm{PE\ chains}} = \frac{x_{\mathrm{PE}}\phi_{\mathrm{PE}}}{\phi_{\mathrm{agg}}}\frac{R_{\mathrm{agg}}^2}{R_{\mathrm{PE}}^2}. \tag{S15}$$

where R_{agg}^2 is the radius of the mixed aggregates and R_{PE}^2 is the radius of an individual PE chain.

The attentive reader may have noticed that the error bars at low Q are rather large for samples with low intensity, especially for the pure JR 400 (see for example figs. S6 and S7). Since only the long wavelength edge of the wavelength band and comparably few pixels close to the beam stop of the detector contribute to the lowest Q points, which reduces the effective incoming flux for these Q values. If these effect are not counter balanced by a strong increase in scattering intensity towards low Q (as for example in the other curves in fig. S6) this results in comparably large error bars at low Q and measuring sufficiently long to have error bars comparable to the other curves with higher intensities at low Q quickly becomes unfeasible.

S IV Neutron Spin-Echo Spectroscopy

NSE directly yields the normalised intermediate scattering function $S(q,t)$, which can usually be approximated with a simple exponential

$$S(Q,t) = \exp(-D_{\mathrm{app}}(Q)Q^2t) \tag{S16}$$

where D_{app} is the Q dependent apparent diffusion coefficient, which is related to the apparent hydrodynamic radius

$$R_{\mathrm{h}}(Q) = \frac{k_{\mathrm{B}}T}{6\pi\eta D_{\mathrm{app}}(Q)} \tag{S17}$$

where k_{B} is the Boltzmann constant, T is temperature and η is the viscosity of the solvent. For non-interacting, spherical particles, R_{h} coincides with the geometrical radiu.

The diffusion of rodlike particles with radius R and length L can be described using the Broersma equation[8]. The translational (D_{rod}) and the rotational (Θ_{rod}) diffusion coefficients are given by:

$$D_{\mathrm{rod}} = \left(\frac{k_{\mathrm{B}}T}{3\pi\eta_{\mathrm{solv}}L}\right)(\delta - 0.5\left[\gamma_{\parallel}(\delta) + \gamma_{\perp}(\delta)\right]) \tag{S18}$$

$$\Theta_{\mathrm{rod}} = \left(\frac{3k_{\mathrm{B}}T}{\pi\eta_{\mathrm{solv}}L^3}\right)(\delta - \zeta(\delta)), \tag{S19}$$

where $\delta = \ln(L/R)$, $\gamma_{\parallel} = 1.27 - 7.4(1/\delta - 0.34)^2$, $\gamma_{\perp} = 0.19 - 4.2(1/\delta - 0.39)^2$ and $\zeta = 1.45 - 7.2(1/\delta - 0.27)^2$. The resulting intermediate scattering has a double exponential decay:

$$S_{\mathrm{rod}}(Q,t) = s_0(Q)\exp(-D_{\mathrm{rod}}Q^2t) + s_1(Q)\exp(-(D_{\mathrm{rod}}Q^2 + 6\Theta_{\mathrm{rod}})t) \tag{S20}$$

with the amplitudes

$$\begin{aligned} s_0(Q) &= \left(\frac{2}{QL}\int_0^{\frac{QL}{2}} j_0(z)\,\mathrm{d}z\right)^2 \\ s_1(Q) &= 5\left(\frac{1}{QL}\left(-3j_1\left(\frac{QL}{2}\right) + \int_0^{\frac{QL}{2}} j_0(z)\,\mathrm{d}z\right)\right)^2 \end{aligned} \tag{S21}$$

where j_n is the n_{th} order spherical Bessel function.

At intermediate length scales, the behaviour of a polymer in solution is governed by hydrodynamic interactions. D_{app} depends linearly on Q and the slope a is related to the solvent viscosity[9–11] so that $D_{\mathrm{app}}(Q) = D_0 + aQ$. Dubois-Violette and De Gennes[11] derived an expression for the intermediate scattering function of an infinitely long polymer in solution based on a Rouse-Zimm

chain[12]:

$$S_{\mathrm{Zimm}}(Q,t) = (\Gamma_{\mathrm{Zimm}}t)^{2/3}\int_0^\infty \exp\left(-(\Gamma_{\mathrm{Zimm}}t)^{2/3}u\,[1+h(u)]\right)\mathrm{d}u \tag{S22}$$

$$S_{\mathrm{Zimm}}(Q,0) = 1$$

$$h(u) = \frac{4}{\pi}\int_0^\infty \frac{\cos(y^2)}{y^3}\left[1-\exp(-y^3u^{-3/2})\right]\mathrm{d}y \tag{S23}$$

where

$$\Gamma_{\mathrm{Zimm}} = \frac{\sqrt{3}Q^3k_{\mathrm{B}}T}{6^{3/2}\eta_{\mathrm{solv}}}, \tag{S24}$$

and the solvent viscosity η_{solv} is the only property of the sample entering in eq. (S22). To account for translational diffusion, eq. (S22) is modified as follows:

$$S^{\mathrm{diff}}_{\mathrm{Zimm}}(Q,t) = \exp(-D_0Q^2t)\left[(1-A(Q))+A(Q)S_{\mathrm{Zimm}}(Q,t)\right], \tag{S25}$$

where $A(Q)$ is the amplitude of the internal motions of the polymer and D_0 accounts for the translational diffusion of the polymer.

The intermediate scattering functions of samples with single-charged surfactant can be described as superposition of S_{rod} (eq. (S20)) and $S^{\mathrm{diff}}_{\mathrm{Zimm}}$ (eq. (S25)) where the ratio between the two contributions is fixed through x_{PE} which is known from the SANS fits. In addition, at long Fourier times, an elastic component becomes visible, which is accounted for by a constant term S_{el}:

$$S(Q,t) = \frac{1}{S(Q,0)}\left(\frac{\phi_{\mathrm{surf}}+x_{\mathrm{PE}}\phi_{\mathrm{PE}}}{V_{\mathrm{agg}}}P_{\mathrm{agg}}\cdot S_{\mathrm{rod}}(Q,t)\right.$$
$$\left.+\frac{(1-x_{\mathrm{PE}})\phi_{\mathrm{PE}}}{V_{\mathrm{PE}}}P_{\mathrm{PE}}\cdot S^{\mathrm{diff}}_{\mathrm{Zimm}}(Q,t)\right)+S_{\mathrm{el}}(Q). \tag{S26}$$

In these fits, the only free parameters are the (Q-independent) length of the rods in $S_{\mathrm{rod}}(Q,t)$ and $S_{\mathrm{el}}(Q)$. All other parameters are either known from SANS or fits to the NSE data of the pure JR 400 solution.

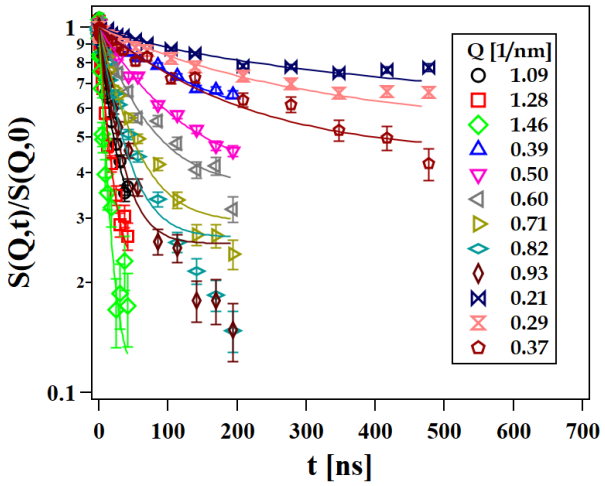

Fig. S9 NSE intermediate scattering functions of PESCs with 1 wt% JR 400 and 5 mM SDP^- ($Z=2$), fits according to eq. (S26).

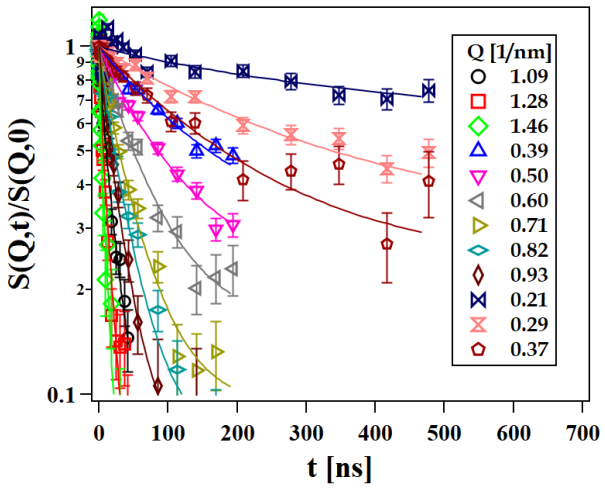

Fig. S10 NSE intermediate scattering functions of PESCs with 1 wt% JR 400 and 2 mM SDP^- ($Z=5$), fits according to eq. (S26).

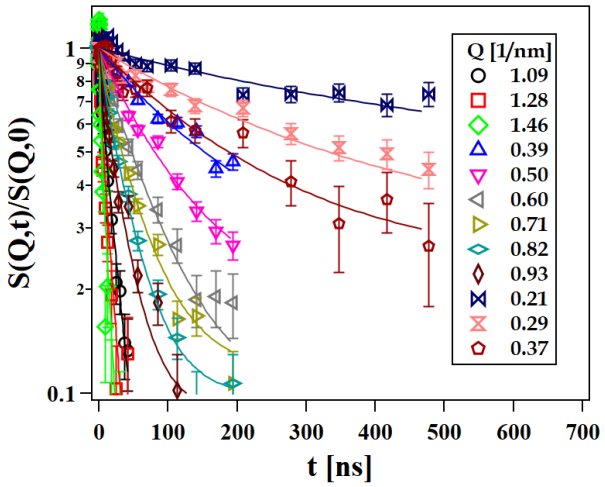

Fig. S11 NSE intermediate scattering functions of PESCs with 1 wt% JR 400 and 1.4 mM SDP^- ($Z=7$), fits according to eq. (S26).

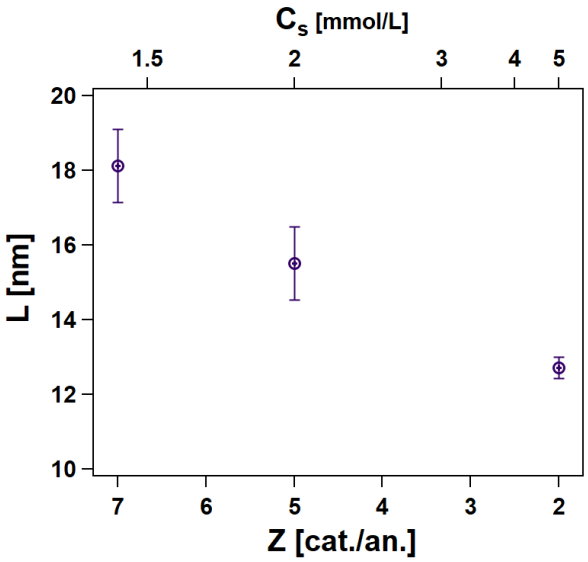

Fig. S12 Length of the mixed rodlike PE/surfactant aggregates for samples with 1 wt% JR 400 and SDP^-. The aggregates become slightly shorter as more surfactant is added.

Notes and references

1 K. Nakayama, I. Tari, M. Sakai, Y. MURATA and G. SUGIHARA, *Journal of Oleo Science*, 2004, **53**, 247–265.

2 P. Walde, M. Wessicken, U. Rädler, N. Berclaz, K. Conde-Frieboes and P. L. Luisi, *The Journal of Physical Chemistry B*, 1997, **101**, 7390–7397.

3 I. Hoffmann, S. Prévost, M. Medebach, S. E. Rogers, N. J. Wagner and M. Gradzielski, *Tenside, Surfactants, Deterg.*, 2011, **48**, 488–494.

4 M. S. Green and A. V. Tobolsky, *The Journal of Chemical Physics*, 1946, **14**, 80–92.

5 J. Smilek, S. Jarábková, T. Velcer and M. Pekař, *Polymers*, 2019, **11**, 927.

6 G. Beaucage, *Journal of Applied Crystallography*, 1995, **28**, 717–728.

7 G. R. Del Sorbo, V. Cristiglio, D. Clemens, I. Hoffmann and E. Schneck, *Macromolecules*.

8 S. Broersma, *J. Chem. Phys.*, 1960, **32**, 1626–1631.

9 D. Richter, M. Monkenbusch, A. Arbe and J. Colmenero, in *Neutron Spin Echo in Polymer Systems*, Springer, 2005, pp. 1–221.

10 A. Akcasu, M. Benmouna and C. C. Han, *Polymer*, 1980, **21**, 866–890.

11 E. Dubois-Violette and P. G. De Gennes, *Phys. (New York)*, 1967, **3**, 181.

12 B. H. Zimm, *J. Chem. Phys.*, 1956, **24**, 269–278.